Molecular Vision 2006; 12:606-15 <http://www.molvis.org/molvis/v12/a67/>
Received 28 February 2005 | Accepted 19 April 2006 | Published 26 May 2006

Construction, gene delivery, and expression of DNA tethered nanoparticles

Tarl Prow,[1,2,3] Jacob N. Smith,[2] Rhonda Grebe,[3] Jose H. Salazar,[2] Nan Wang,[2] Nicholas Kotov,[4] Gerard Lutty,[3] James Leary[1,2,5]

Departments of [1]Pathology and [2]Infectious Diseases, University of Texas Medical Branch, Galveston, TX; [3]The Wilmer Ophthalmologic Institute, Department of Ophthalmology, The Johns Hopkins Hospital, Baltimore, MD; [4]Department of Chemical Engineering, University of Michigan, Ann Arbor, MI; [5]Basic Medical Sciences and Biomedical Engineering, Purdue University, West Lafayette, IN

Purpose: Layered nanoparticles have the potential to deliver any number of substances to cells both in vitro and in vivo. The purpose of this study was to develop and test a relatively simple alternative to custom synthesized nanoparticles for use in multiple biological systems, with special focus on the eye.
Methods: The biotin-labeled transcriptionally active PCR products (TAP) were conjugated to gold, semiconductor nanocrystals, and magnetic nanoparticles (MNP) coated with streptavidin. The process of nanoparticle construction was monitored with gel electrophoresis. Fluorescence microscopy followed by image analysis was used to examine gene expression levels from DNA alone and tethered MNP in human hepatoma derived Huh-7 cells. Adult retinal endothelial cells from both dog (ADREC) and human (HREC) sources were transfected with nanoparticles and reporter gene expression evaluated with confocal and fluorescent microscopy. Transmission electron microscopy was used to quantify the concentration of nanoparticles in a stock solution. Nanoparticles were evaluated for transfection efficiency, determined by fluorescence microscopy cell counts. Cells treated with MNP were evaluated for increased reactive oxygen species (ROS) and necrosis with flow cytometry.
Results: Both 5' and 3' biotin-labeled TAP bound equally to MNP and there were no differences in functionality between the two tethering orientations. Free DNA was easily removed by the use of magnetic columns. These particles were also able to deliver genes to a human hepatoma cell line, Huh-7, but transfection efficiency was greater than TAP. The semiconductor nanocrystals and MNP had the highest transfection efficiencies. The MNP did not induce ROS formation or necrosis after 48 h of incubation.
Conclusions: Once transfected, the MNP had reporter gene expression levels equivalent to TAP. The nanoparticles, however, had better transfection efficiencies than TAP. The magnetic nanoparticles were the most easily purified of all the nanoparticles tested. This strategy for bioconjugating TAP to nanoparticles is valuable because nanoparticle composition can be changed and the system optimized quickly. Since endothelial cells take up MNP, this strategy could be used to target neovascularization as occurs in proliferative retinopathies. Multiple cell types were used to test this technology and in each the nanoparticles were capable of transfection. In adult endothelial cells the MNP appeared innocuous, even at the highest doses tested with respect to ROS and necrosis. This technology has the potential to be used as more than just a vector for gene transfer, because each layer has the potential to perform its own unique function and then degrade to expose the next functional layer.

The majority of nanoparticle research, to date, has been carried out by materials scientists, but recent trends have brought these tools into the hands of biologists. Nanoparticles have found two broad niches in biology, detection technologies and payload delivery [1,2]. Since the late 1970s, nanoparticles have been used to deliver drugs [2,3]. In fact, the majority of publications concerning biological applications of nanoparticles are focused on the delivery of chemotherapeutic agents with nanoparticles ranging from 2 to 3000 nm. Nanoparticle mediated gene delivery has recently emerged as a promising tool for gene therapy strategies [4-6]. The main problems with using nanoparticles for gene delivery are the construction, cost, and quality control of the nanoparticles themselves. The construction quickly becomes very complicated when the number of layers increases. This is due to the interactions between layers and between nanoparticles with incomplete and complete layering. These factors limit the usefulness of nanotechnology to laboratories that have chemists capable of nanoparticle synthesis or to investigators in collaboration with chemists. This limits the technology, especially for small laboratories. This study documents the development of a streptavidin nanoparticle system that is simple and quite flexible from a commercially available product intended for other uses.

Magnetic nanoparticles have been primarily applied to three fields: magnetic resonance imaging, molecular and cell separation technologies, and drug delivery [7-11]. Many researchers use magnetic particles as contrast agents [12-16].

Correspondence to: James Leary, Basic Medical Sciences and Biomedical Engineering, Purdue University, West Lafayette, IN, 47907; Phone: (765) 494-7280; FAX: (765) 496-6443; email: jfleary@purdue.edu

Because these agents are used primarily in diagnostic in vivo imaging, many of the particle formulations are already approved for use in humans. The magnetic properties of these particles are quite favorable for layered construction of a nonviral based gene delivery vector.

We are currently developing a nanomedicine strategy to prevent retinopathy of prematurity (ROP) [17], a disease in which it would be undesirable to use a viral gene delivery system in premature infants. Our strategy is to deliver a nanoparticle to a cell in the eye that is capable of detecting and reacting to the initial hyperoxic insult that is the first stage of ROP, vaso-obliteration [17]. This event will trigger the expression of a therapeutic gene able to save the cells in the eye that would normally die and leave the retina with a compromised vasculature. Before this can be accomplished, however there are many challenges to overcome.

One of the most difficult challenges facing researchers constructing layered nanoparticles is the purification of the particles after each step. With magnetic particles, the purification is generally simple and utilizes magnetic columns. The magnetic properties of nanoparticles have been used to enhance gene transfer for gene therapy applications [18-22]. In this case, the nanoparticles were used to concentrate the plasmid to a specific location and thereby increase the likelihood of transfection [22]. The Plank lab used clusters of plasmid DNA and coated magnetic nanoparticles were used to target cells using the magnetic properties of the nanoparticle clusters [18].

Several nanoparticle cores were investigated in this study, including gold, semiconductor nanocrystals, and magnetic iron oxide. Gold nanoparticles have traditionally been used as for immunolabeling in transmission electron microscopy and are commercially available in a variety of sizes. We chose to evaluate one of the smaller gold nanoparticles (5 nm) available with streptavidin already conjugated to the surface. Semiconductor nanocrystals are about 25 nm in diameter and have very unique optical properties. These nanoparticles do not photobleach, fluoresce intensely with UV excitation, and are capable of having streptavidin bioconjugated to their surface [23].

Superparamagnetic nanoparticle cores coated with dextran bioconjugated to streptavidin were chosen for gene transfer because they were easily obtainable, simple to construct and could be purified from the unbound layer components using magnetic columns. The core particles are composed of an iron oxide core coated with dextran and bioconjugated to streptavidin, with the complete particle measuring approximately 100 nm in diameter. We have developed a simple procedure for DNA conjugation, purification, and delivery to cells. These particles were found to have reasonable transfection efficiency, with respect to free DNA, when coated with lipid. Genes were expressed from magnetic nanoparticles at levels slightly below that of free DNA. Magnetic nanoparticles were capable of transfecting several cell types including an immortalized human hepatoma cell line, Huh-7, and adult retinal endothelial cells from both dog (ADREC) and human (HREC) sources. This study demonstrates that the magnetic and semiconductor nanoparticles were the two largest and most efficient for transfecting ADREC. Finally, the magnetic nanoparticles alone did not induce oxidative stress or necrosis as determined by flow cytometry.

METHODS

Biotin-labeled DNA fragment preparation: PCR amplification was used to create biotin-labeled DNA fragments. Oligonucleotide primers were purchased from Integrated DNA Technologies, Inc. For initial studies, either the 5' or the 3' oligo was made with a single biotin tag. The sequences were based

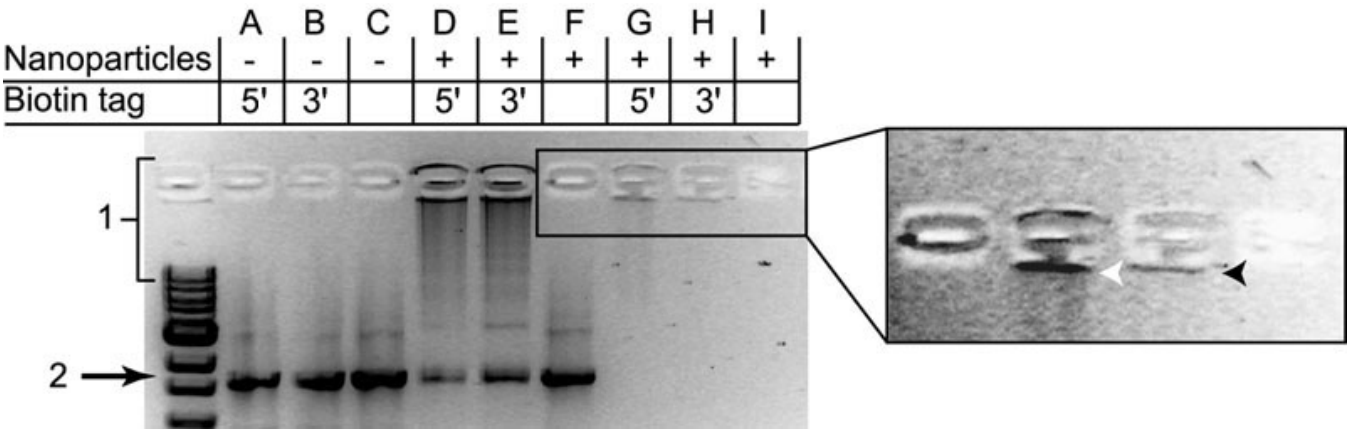

Figure 1. Construction and purification of DNA tethered magnetic nanoparticles. Gel electrophoresis was used to examine the successful construction of the DNA tethered magnetic nanoparticles and to verify that the purification removed the unbound DNA from the nanoparticles. Lanes A-C represent only DNA fragments. Lanes D-F contain the MNP/DNA mixture. After washing with a magnetic column, a portion of the purified MNP were also run on this gel (Lanes G-I). On the right is a magnified image of the box around Lanes F-I. This gel shows three critical stages of nanoparticle construction, DNA alone, DNA tethered nanoparticle in excess DNA, and finally DNA tethered nanoparticles free of unbound DNA.

on the pEGFP-C1 (BD Clontech, Inc., Mountain View, CA) template: forward 5'-TAG TTA TTA ATA GTA ATC AAT TAC GGG GTC ATT AG-3', reverse 5'-TAC ATT GAT GAG TTT GGA CAA ACC ACA ACT AGA AT-3' (Integrated DNA Technologies, Inc., Coralville, IA). The forward primer begins on the first nucleotide of the CMV promoter (red thymine), whereas the reverse primer is past the last nucleotide of the SV40 polyadenylation signal. Thus all of the components necessary for gene expression are present in the PCR product. Later studies used only 5' oligonucleotides labeled with biotin. These oligonucleotides were then used as PCR primers. A typical reaction would include 25 µl Red Taq, (Sigma, Inc., St. Louis, MO), 1 µl 5' biotinylated primer, 1 µl 3' primer, 1 µl template, to 50 µl with water. The primers were at 200 pM and the template at 50 ng/µl. A typical reaction for DNA tethering to magnetic nanoparticles would include 25 of these reactions combined. Typical PCR cycles would include about 35 cycles of denaturing temperature at 94 °C for 30 s, annealing temperature at 65 °C for 30 s and extension for 2 min at 72 °C.

DNA tethered nanoparticle construction: Biotin-labeled PCR products were tethered to streptavidin-coated magnetic nanoparticles (Miltenyi Biotech, Inc., Auburn, CA). This nanoparticle has an iron oxide core coated with dextran that is bioconjugated to streptavidin. DNA tethered magnetic nanoparticles were constructed by incubating the magnetic nanoparticles with the biotin-labeled PCR fragments at the ratio of 31 ng DNA to 1 µl of nanoparticles. The mixture was incubator at room temperature for 30 min. During that time, the magnetic column was prepared by washing once with the 100 µl of the nucleic acid buffer and three times with 100 µl of Optimem (Gibco, Inc., Rockville, MD). Once washed, the column was loaded with the DNA nanoparticle mixture. The column was then washed three times with 100 µl Optimem. The nanoparticles were eluted by removing the column from the magnet and adding the 100 µl of Optimem. The resulting brownish solution contained DNA tethered nanoparticles.

The amount of transcriptionally active PCR products (TAP) bound per µl of streptavidin-Cy3 (SA), gold nanoparticles (GNP), nanocrystals (NC; made by the Kotov lab or purchased from Quantum Dot, Inc., Hayward, CA), and MNP was determined by gel electrophoresis. An excess of TAP was added to 10 µl of the nanoparticle stock solution and incubated at room temperature for 20 min. The maximal

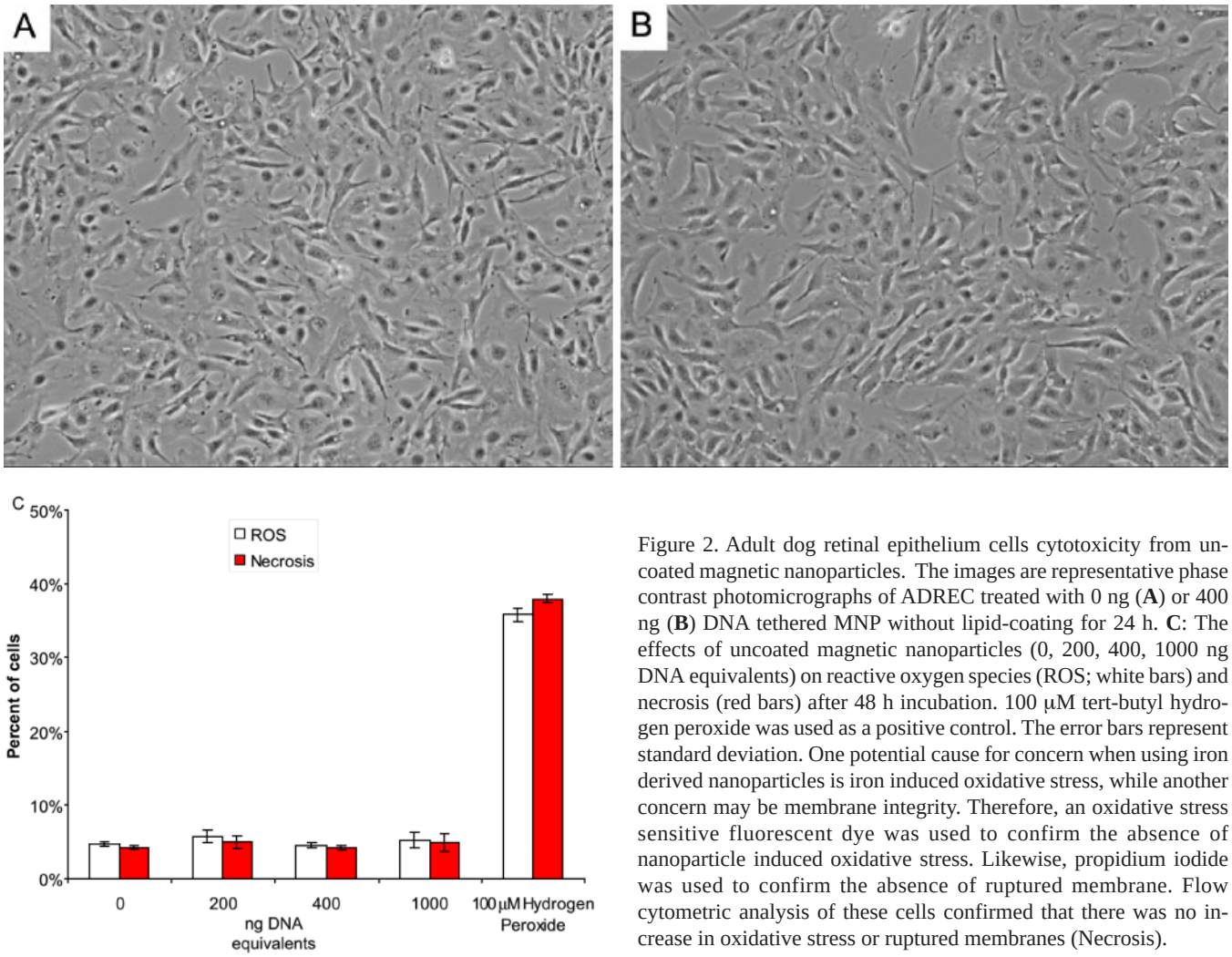

Figure 2. Adult dog retinal epithelium cells cytotoxicity from uncoated magnetic nanoparticles. The images are representative phase contrast photomicrographs of ADREC treated with 0 ng (**A**) or 400 ng (**B**) DNA tethered MNP without lipid-coating for 24 h. **C**: The effects of uncoated magnetic nanoparticles (0, 200, 400, 1000 ng DNA equivalents) on reactive oxygen species (ROS; white bars) and necrosis (red bars) after 48 h incubation. 100 µM tert-butyl hydrogen peroxide was used as a positive control. The error bars represent standard deviation. One potential cause for concern when using iron derived nanoparticles is iron induced oxidative stress, while another concern may be membrane integrity. Therefore, an oxidative stress sensitive fluorescent dye was used to confirm the absence of nanoparticle induced oxidative stress. Likewise, propidium iodide was used to confirm the absence of ruptured membrane. Flow cytometric analysis of these cells confirmed that there was no increase in oxidative stress or ruptured membranes (Necrosis).

amount of TAP bound per μl of SA, GNP, NC, and MNP was determined by semi-quantitative gel electrophoresis to be 37.4, 16.9, 54.4, and 31.1 ng per μl, respectively. Therefore, 100 ng TAP would bind 2.7 μl SA, 5.9 μl GNP, 1.8 μl NC, and 3.2 μl MNP.

Lipid coating of DNA tethered magnetic nanoparticles: The DNA tethered nanoparticles (400 ng DNA/13 μl MNP) were coated with Lipofectamine 2000. The eluted particles were diluted in the 250 μl of Optimem and incubated for 5 min at room temperature. 10 μl of Lipofectamine 2000 was diluted with 250 μl of Optimem in a separate tube and incubated at room temperature for 5 min. After 5 min, the two tubes were mixed gently and combined. This mixture was allowed to stand for 20 min before adding to the cell culture. All nanoparticles had lipid coating except those in Figure 1, Figure 2B, and Figure 3 (as noted on the x-axis).

Confocal and fluorescence microscopy: Cells were examined for reporter gene expression with a Zeiss 510META confocal microscope. The two types of nanocrystals used for these studies had 525 and 565 nm emission peaks. After excitation with a 405 nm diode laser the emission light was passed through a 490 nm long pass filter and finally detected with 520 nm and 560 nm bandpass filters for the 525 and 565 nm nanocrystals, respectively. EGFP was excited with a 488 nm argon ion laser and the emission light was passed through a 490 nm long pass filter and finally detected with a 520 nm bandpass filter. DsRed was excited with a 543 nm HeNe laser and the emission light was passed through a 490 nm long pass filter and finally detected with a 560 nm bandpass filter. Differential interference contrast (DIC) microscopy was also used to image all cells using the 488 nm argon ion line.

Fluorescence microscopy was performed using a Nikon Eclipse TE2000-U inverted microscope. Photomicrographs were taken with a SPOT RT SE digital camera, Diagnostic Instruments, Inc. (Sterling Heights, MI). Nanocrystals were imaged using a Nikon Fluorogold filter set, which excites with UV and contains a 505 nm long pass emission filter. EGFP was imaged with a standard Nikon FITC filter set, while DsRed was imaged using a standard Nikon Cy3 filter set.

Image analysis for gene expression levels: A standard wave-propagation algorithm was used to segment the images over a singular threshold. Upper and lower boundaries were chosen for subsegmentation. Segments which fell below the lower area bound were removed. Segments which were above the upper boundary were re-segmented with a higher threshold and reexamined. The threshold level was computed as the average of the intensity of the pixels within the segment minus the standard deviation of the intensity of the pixels bounded below by zero. Threshold levels are computed individually for each subsegment. The output is a list of segments associated with a bitmap representing the segment, the total intensity, area, and standard deviation of intensity for that segment [24].

Cell culture: Cells were incubated at 37 °C in 5% CO_2. The Huh-7 cell line, derived from a human hepatoma (gift from Rene Rijnbrand, University of Texas Medical Branch, Galveston, TX), was cultured in DMEM supplemented with 10% FBS (Sigma, Inc.) and penicillin/streptomycin (Sigma).

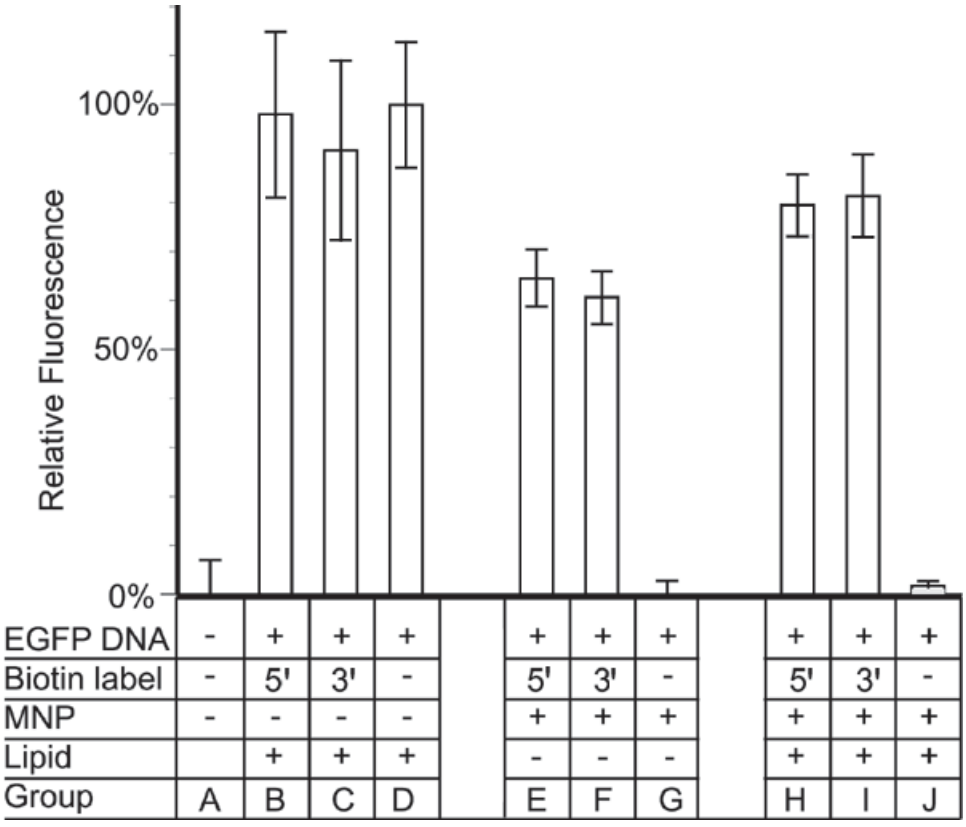

Figure 3. Expression levels of enhanced green fluorescent protein from lipid-coated and uncoated DNA tethered magnetic nanoparticles. In vitro gene expression levels are shown as the percentage of lipofectamine-transfected enhanced green fluorescent protein DNA. Biotin tagged DNA was also transfected into cells. All samples were incubated with or without lipofectamine 2000.

Each experiment was done at least in triplicate and positive and negative controls were present in all experiments.

Primary cell lines of ADREC were established as reported by Lutty et al. [25]. Adult beagles were euthanized by an intraperitoneal overdose of pentobarbital sodium. Animals were treated in accordance with the ARVO Statement for the Use of Animals in Ophthalmic and Vision Research. The eyes were enucleated and placed in cold, sterile PBS and excess tissue was cleared away. The eyes were then soaked in cold Betadine for 15 min. The retina was washed thoroughly and homogenized in PBS, with a Dounce homogenizer. The homogenate was filtered with a 105 μm Nitex nylon mesh in a porcelain funnel under a gentle vacuum. The filtrate was then passed through a 58 μm Nitex mesh. The vessel retentate was digested in 0.375% collagenase and 0.25% bovine serum albumin in PBS for 45-60 min at 37 °C. The digestion was then stopped by the addition of DMEM/F12 media supplemented with 10% fetal bovine serum, 1% penicillin/streptomycin/fungizone (Gibco, Inc.). The cells were then incubated at 37 °C in 5% CO_2 for 24 h in a T-25 flask. After 24 h, the unattached cells and debris were washed away and the remaining cells were fed fresh media. All studies were done with cells at less than passage 10. The endothelial cells used in these studies were vWF positive and took up Acetylated LDL.

Human retinal endothelial cells were purchased from Cell Systems, Inc. (Kirkland, WA). These cells were maintained on CSC medium from Cell Systems, Inc. Later, however, the cells were successfully grown and split in the same fashion and with the same medium as the ADREC above.

Cytotoxicity of magnetic nanoparticles: Cytotoxicity was evaluated by morphological analysis of ADREC incubated with MNP for 24 h at several concentrations including, 0, 200, 400, 4000, and >15,000 ng of DNA. After incubation, the cells were photographed under phase illumination as described above. Reactive oxygen species formation after nanoparticle treatment was determined by treating AREC with 0, 200, 400, and 1000 ng DNA equivalents of MNP (nanoparticles without DNA or lipid coating) for 48 h. After incubation with the nanoparticles, the cells were washed three times in PBS and trypsinized to attain a cell suspension and stained with 50 μm/ml propidium iodide (Sigma) for 10 min in DMEM/F12 at 37 °C in 5% CO_2. After staining the cells were washed three times with PBS. Next, the cells were stained with 5-(and 6-)chloromethyl-2',7'-dichlorodihydrofluorescein diacetate, acetyl ester (CM-H_2DCFDA) in DMEM/F12 at 5 μM for 30 min under culture conditions. After CM-H_2DCFDA staining, the cells were washed three times in PBS and trypsinized to attain a cell suspension. The cells were then washed three times in complete media without phenol red. As a positive control some cells were treated with 100 μM tert-butyl hydrogen peroxide for 30 min prior to staining. The cells were analyzed on a FACScalibur flow cytometer, and data were analyzed by CellQuest software (both from Becton Dickinson Immunocytometry Systems, San Jose, CA).

Magnetic nanoparticle quantification with transmission electron microscopy (TEM): The stock solution of MNP was purchased from Miltenyi Biotech, Inc. MNP stock solution (10 μl) was diluted 1:100,000 with PBS. The diluted MNP were then incubated with ten μl of biotin coated polystyrene beads (1.75 million beads, 3.27 μm diameter from Spherotech, Inc., Libertyville, IL) in 990 μl of PBS for 30 min at room temperature. After 30 min, the beads were washed three times in PBS by centrifugation at 1500 RPM in a Beckman TJ-6 centrifuge with a TH-4 1-88 rotor for 5 min. After washing, the beads were fixed in fresh, 2% paraformaldehyde for 10 min. The beads were then dried overnight in a Savant SpeedVac concentrator SVC100H. The beads were then mixed with LX112 polymer (Ladd Research Industries, Inc., Burlington, VT) and the solution placed in a cylindrical block mold in a heated block form (Pelco International, Inc., Redding, CA) and polymerized at 60 °C for 36 h. Thin sections (95 nm) were cut on a Leica Ultracut UTC ultramicrotome and collected on 150 mesh uncoated copper grids. Samples were viewed and photographed with a JEOL 100CX TEM (JEOL USA, Inc., Peabody, MA). NIH Image was used to determine the area of the bead (n=90). The area and section thickness of the beads were used to calculate the surface area of the cylinder ($2\pi r^2$) exposed to nanoparticles. Nanoparticles were also quantified and the data used to calculate the number of nanoparticles per micrometer squared. This was then used to determine the number of nanoparticles per μl (40 million).

RESULTS

Conjugation of DNA to magnetic nanoparticles: Biotin-labeled PCR primers were used to generate CMV-EGFP-pA (CMV promoter, EGFP reporter gene, and poly A signal) containing DNA fragments (1.5 kb) with 5' biotin-labeled, 3' biotin-labeled, or unlabeled. Streptavidin-coated magnetic nanoparticles were incubated with each of the DNA fragments, and no Lipofectamine, and analyzed by agarose gel electrophoresis (Figure 1). Figure 1 lanes A to C contained only the PCR product. Figure 1 lanes D and F contained magnetic nanoparticles incubated with the PCR fragments. DNA in Figure 1 lanes C and F contained no biotin tag and were, therefore, used as negative controls. The black square indicates increased molecular weight DNA. The dark staining seen at the top of Figure 1 lanes D and E indicate that the DNA was able to bind to magnetic nanoparticles and was now trapped at the top of the gel due to its large size. This gel also shows that there is a significant amount of unbound DNA present. Because of this, the magnetic nanoparticles need to be purified from the contaminating free DNA fragments as described in the next section.

The MNP's were the only nanoparticles capable of being easily separated from unbound DNA. Therefore, the other streptavidin-tagged nanoparticles used in this study had to be incubated with the correct amount of DNA so as to avoid nanoparticles without DNA and free DNA. This binding ratio of nanoparticle to DNA was determined for each nanoparticle and streptavidin by semiquantitative gel electrophoresis (data not shown). Nanoparticles and streptavidin were individually incubated with a known excess of 5' biotin labeled TAP. This mixture was then electrophoresed on an agarose gel similar to that shown in Figure 1. The amount of unbound TAP was de-

termined in a semiquantitative nature. The maximal amount of TAP bound per µl of SA, GNP, NC, and MNP was determined by semi-quantitative gel electrophoresis to be 37.4, 16.9, 54.4, and 31.1 ng per µl, respectively. Therefore, 100 ng TAP would bind 2.7 µl SA, 5.9 µl GNP, 1.8 µl NC, and 3.2 µl MNP.

Removal of free DNA from magnetic nanoparticle/DNA solutions: In these experiments, the mixtures of DNA and magnetic nanoparticles were washed four times to remove unbound DNA using a magnetic column. It was found that the magnetic properties of these particles enabled the rapid purification of the magnetic nanoparticles from the DNA solution. These samples were then run on an agarose gel (Figure 1). Figure 1 lanes A and C represent only DNA fragments. Figure 1 lanes D and F contain the magnetic nanoparticle/DNA mixture. After washing, a portion of the magnetic nanoparticles were run onto this gel (Figure 1 lanes G and I). If carefully examined (inset) dark staining can be seen only in Figure 1 lanes G and H near the loading well. This suggests that the free DNA has been removed and only the DNA tethered magnetic nanoparticles remain in solution.

Cytotoxicity of uncoated magnetic nanoparticles in adult dog retinal endothelial cells: Adult dog retinal endothelial cells (ADREC) were treated with increasing concentrations of non-lipid-coated MNP and examined for signs of cytotoxicity. As seen in Figure 2, there are no differences in cells

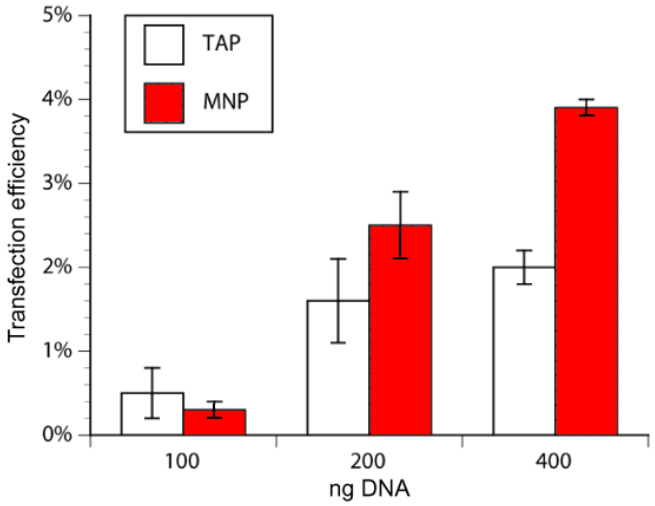

Figure 4. Transfection efficiencies of lipid-coated magnetic nanoparticles in adult dog retinal endothelial cells. Three different concentrations of transcriptionally active PCR products (TAP; white bars) were used (100, 200, and 400 ng per well of 24 well plates) either alone or tethered to lipid-coated nanoparticles (MNP; red bars). Approximately 1000 cells were analyzed for each data point. The bars represent the mean of 3 wells; the error bars represent the standard error of the mean. These data show that TAP tethered magnetic nanoparticles are better at transfecting cells than free TAP in the 200 and 400 ng groups.

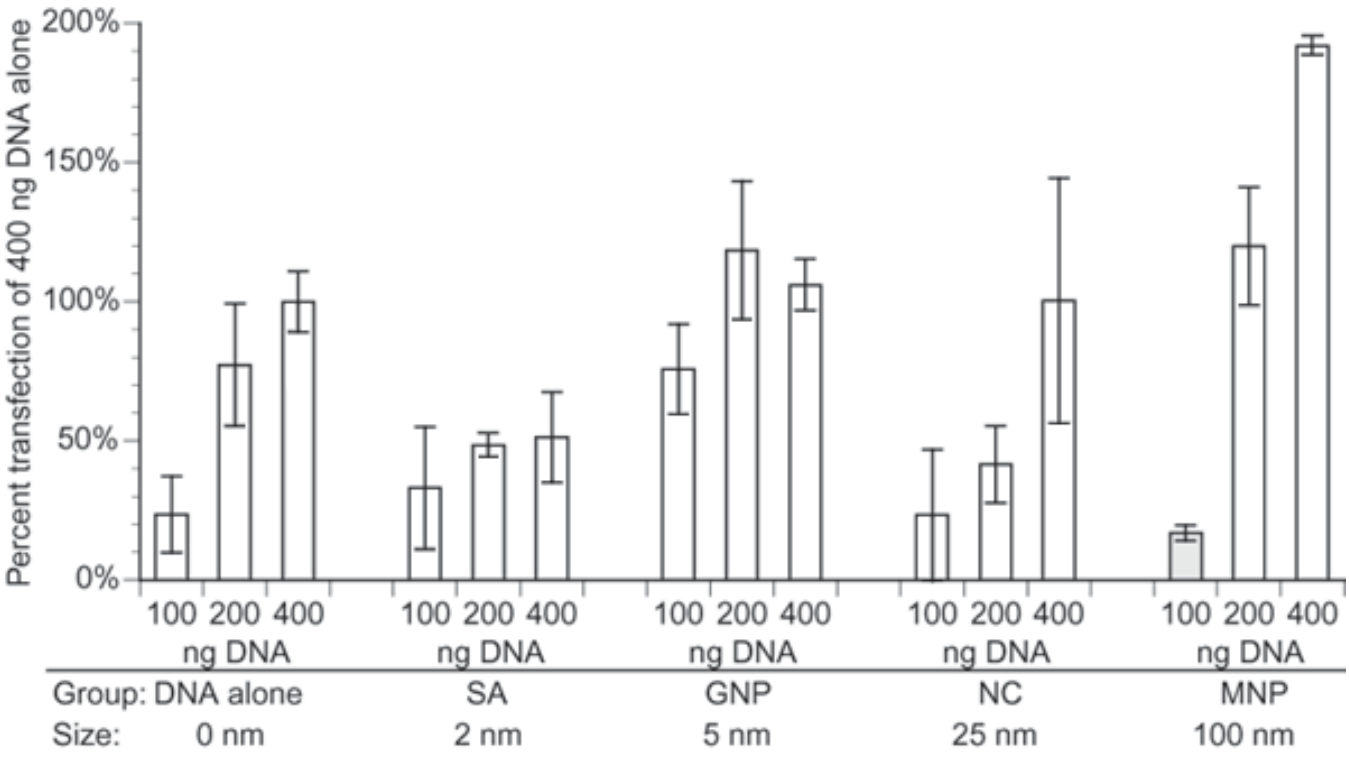

Figure 5. Transfection efficiencies of multiple lipid-coated nanoparticle sizes and cores. Five transfection groups, including DNA alone, streptavin-Cy3 (SA), 5 nm gold nanoparticles (GNP), 25 nm semiconductor nanocrystals (NC), and 100 nm magnetic nanoparticles (MNP), were tested at three different DNA concentrations (100, 200, and 400 ng). All values were normalized to the 400 ng DNA alone group and all groups were coated with lipid. The 400 ng MNP group had statistically significant greater transfection ($p<0.01$), when compared to the 400 ng DNA alone, SA, GNP, or the NC groups using the Student's t-test.

exposed to MNP versus the untreated control. There are no apparent signs of cytotoxicity, including pycnosis, blebbing, or detachment. All of these cells appeared normal from the beginning of the experiment to the end and were treated with several concentrations of MNP ranging from 0 to the stock concentration (40 million MNP per μl), which was dark brown. Uncoated magnetic nanoparticles with no lipid coating were tested for their ability to induce ROS formation or necrosis in ADREC after incubation for 48 h. One hundred μM tert-butyl hydrogen peroxide was added to the cells for 30 min prior to flow cytometric analysis and was used as a positive control. The results from this experiment are summarized in the graph in Figure 2C. The three groups of cells treated with nanoparticles were equivalent to the untreated control (0) with respect to both ROS and necrosis. The positive control values were substantially greater than any of the treatment groups. In fact in all of the treatment groups, the number of positive cells was approximately 5%.

Expression levels of cells transfected with lipid-coated and non-lipid-coated DNA tethered magnetic nanoparticles: This experiment was designed to assess the ability of the cellular machinery to properly express a protein from a nanoparticle tethered gene. This experiment reveals the level of gene expression as measured by fluorescence microscopy, not to be confused with transfection efficiency, which is discussed later. Different combinations of DNA, biotin labeling, MNP, and lipid coating were tested for their effects on gene expression. The lipid coating has previously been shown to

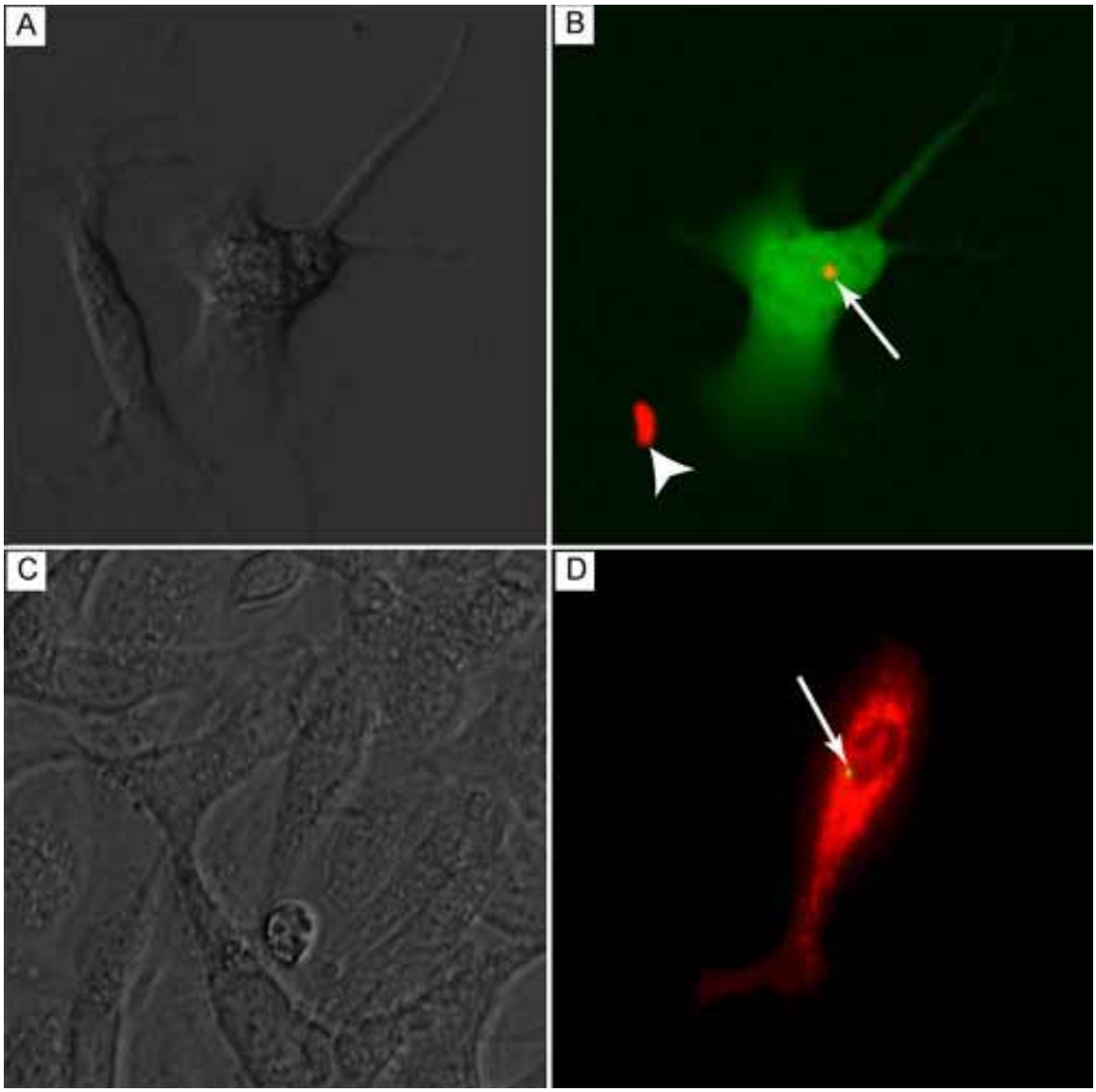

Figure 6. Lipid-coated nanocrystal transfected human retinal epithelium cells. Cells were cultured with lipid-coated nanocrystals tethered to either EGFP (green in **B**) or DsRed (red in **D**) for 48 h or 10 days, respectively. Confocal (**A**,**B**) and fluorescence (**C**,**D**) microscopy were used to simultaneously visualize nanocrystals and tethered fluorescent gene expression. The nanocrystals are marked by white arrows and nanocrystal aggregate is marked with a white arrowhead. **A**: DIC microscopy. **C**: Phase contrast microscopy.

dramatically increase transfection efficiency with naked DNA [26]. The MNP-DNA-Lipid complex was then delivered to Huh-7 cells cultured in chamber slides, incubated for 48 h. The cells were then photographed and the images obtained were then analyzed with an in house slide based cytometry software program (written by JNS, UTMB) and the resulting data presented in Figure 3. All of the values were normalized to the samples treated with the non-biotinylated GFP fragment transfected with Lipofectamine 2000. The labeling of the DNA did not affect the expression of EGFP, as shown in Figure 3 groups B and D. When the DNA was bound to the nanoparticles (Figure 3 groups E and F), there was a decrease in expression levels when compared to naked DNA alone (Figure 3 groups B and C). Figure 3 groups G and J were controls for the construction of the nanoparticles, in that, without a biotin tag the TAP cannot bind the nanoparticle and should be washed away during construction. Indeed, we found that the gene expression levels of Figure 3 groups G and J were equivalent to the true negative control, Figure 3 group A. The intact pEGFP-C1 plasmid was found to have about two times greater expression level than the TAP fragment. This is possibly due to the degradation of the TAP due to the free ends and more substantial transcriptional machinery-binding site.

Transfection efficiencies of lipid-coated magnetic nanoparticles in adult dog retinal endothelial cells: Transfection efficiencies were also determined for different amounts of DNA so that comparisons to naked DNA could be made. The MNP with lipid coating, were evaluated for dose responsiveness and compared to TAP only transfections (Figure 4). The chosen dosages were nanograms of DNA (100, 200, and 400 ng) transfected over 1 h. The majority (>90%) of the transfection occurs in less than 1 h after exposure to MNP (data not shown). The percentage of DsRed positive cells was determined 24 h after transfection. Both the TAP and MNP groups showed a dose dependent increase in transfection efficiency. The MNP showed greater average transfection efficiency than TAP treated cells, in the 200 and 400 ng groups. The MNP groups were less variable than the TAP treated cells.

Transfection efficiencies of different lipid-coated nanoparticles: Transfection efficiency in ADREC was used to determine the optimal size and core material for future nanoparticle experiments. Growing cells were treated with SA, GNP, NC, and MNP all tethered to DNA encoding DsRed and all coated with lipid. As a control, a DNA only group was also run. Forty eight h after exposure, the cells exposed to naked DNA, nanocrystals, and MNP had the highest transfection efficiency (Figure 5). MNP clearly had the best transfection efficiency, at 2 times the naked DNA control in the highest dose (400 ng DNA). All transfection efficiencies were normalized to DNA alone (400 ng DNA, at 10% of the total cells), because this is the most appropriate comparison.

Lipid-coated semiconductor nanocrystal transfection of adult dog retinal endothelial cells: The ability of lipid-coated semiconductor based nanocrystals as potential gene carriers was tested first in ADREC and later in HREC. Confocal imaging of these transfected cells (Figure 6) demonstrated that this nanoparticle was capable of delivering genes to human cells. One interesting observation was that gene expression from nanocrystals transfected cells appeared to be very high in the first 24 h when compared to the DNA alone transfected cells. This was observed in both ADREC and HREC. The downside of using nanocrystals in this way is that purification between construction steps is difficult at best. One of the problems that has plagued the use of nanocrystals is their tendency to form aggregates (Figure 6B, arrowhead). When we attempted to purify the nanocrystals by centrifugation, there was an increase in aggregate formation, so for these studies, the nanocrystals were not purified away from free DNA.

Quantification of magnetic nanoparticles with TEM: Transmission electron microscopy was used to determine the number of MNP in 10 µl of MNP stock solution. The MNP were bound to biotin-coated polystyrene beads and then embedded for analysis. Ninety bead sections were analyzed for the presence of bound nanoparticles and bead area. The bead area was found to have a normal distribution. Because the thickness of the bead section, the amount of nanoparticles and beads added to the mixture were known, we were able to determine the number of nanoparticles per µl. Additionally, it was determined that 3.2 µl of MNP to bind 100 ng of TAP, therefore, it is possible to enumerate the approximate number of TAPS bound per MNP, 47. Finally, 128 million nanoparticles can bind approximately 100 ng of TAP.

DISCUSSION

These studies have demonstrated that lipid-coated nanocrystals and MNP can be used to transfect a variety of cell types including retinal vascular endothelial cells; however, MNP are easier to purify. Construction of these nanoparticles using the streptavidin-biotin conjugation can also be monitored with gel electrophoresis. Magnetic nanoparticles were the most efficient gene delivery vectors tested. Cells incubated with these particles showed no visible signs of toxicity (blebbing, apoptosis, etc.), even though the particles are made of iron. The MNP offer the most promise of the nanoparticles evaluated.

DNA fragments with 5' or 3' biotin tags were attached to streptavidin coated magnetic nanoparticles. Free DNA fragments were successfully removed by washing the particles using a magnetic column. These data indicated that without lipid coating, there were slightly decreased levels of EGFP reporter expression when compared to those MNP with lipid. This may be a result of the number of nanoparticles entering the nucleus. The addition of lipid to transfection solutions is a widely recognized method to increase the amount of DNA that reaches the nucleus. This is also likely to be true for the MNP.

One important finding is that the DNA tethered magnetic nanoparticles not coated with lipid were able to successfully transfect cells in vitro. This result shows that the size range of these particles is appropriate. Another interesting result is that cells treated with the DNA tethered magnetic nanoparticles coated with lipid had expression levels well within range of those transfected with only labeled DNA fragments. These data show that we can effectively express gene products from DNA

tethered to magnetic nanoparticles in either the 5' or 3' configuration. Finally, the unlabeled DNA exposed magnetic nanoparticles that were subsequently washed with a magnetic column, did not show any appreciable expression of GFP. Therefore, the expression we observed with the labeled DNA and magnetic nanoparticles was from DNA tethered to magnetic nanoparticles.

One way to improve the transfection efficiency is to eliminate defective or incomplete nanoparticles prior to delivery. This scenario would explain the differences in transfection seen in this study. This further underscores the importance of nanoparticle purification during construction, one of the main benefits of using MNP. Secondly, although the cellular mechanisms at work are not known, our results suggest that while the nanoparticles get close to the nucleus, most never get in (data not shown). This problem could be solved or at least ameliorated by the addition of targeting molecules to the nanoparticle. However, with the addition of another layer comes the problem of how to purify only the nanoparticle with all of the layers.

Another benefit of this technology is the ability to transfect cells with low concentrations of DNA. The lower limits of this technology are often overlooked and researchers tend to examine maximal doses rather than minimal doses in order to show the best case scenario. These studies often utilized conditions that can never be achieved in live animals. We chose to examine the lower limits of MNP compared to DNA alone to directly compare the two methods of gene transfer. These data demonstrate a distinct advantage by the MNP at the 200 and 400 ng doses (Figure 4). This argument is further strengthened by the fact that there are about 40 times more DNA particles in the TAP treated cells. There are thought to be approximately 47 biotin-binding sites per nanoparticle. If each copy of DNA in the TAP group is considered a particle capable of transfection, then, on a per particle basis, the particles of DNA in the TAP alone group out number the MNP particles 40 to 1. This means that the MNP are much more efficient at transfection than TAP. Even so, the critical factor is the total volume that will be delivered to the eye. Given the size of the premature infant eye or neonatal dog eye, our model of ROP, it is possible to inject 50 μl into the vitreous without having to remove any of the vitreous body. In these studies we have kept the nanoparticle solutions very dilute. This was primarily due to the costs of the reagents. Therefore, the 50 μl target volume should be capable of delivering more than enough nanoparticles, 20 billion MNP or almost 1 trillion copies of the gene, to an individual eye. Reduction of the nanoparticle size would allow for more nanoparticles and more efficient construction could yield an increase in the number of usable DNA strands per nanoparticle.

Another point of contention in the field of nanoparticle based gene delivery is the optimal size and material of the nanoparticles. Our personal experience has guided us to nanoparticles less than 200 nm in diameter. The current study included nanoparticles from 0 (naked DNA) to 100 nm. Although the materials were different, there seemed to be a clear correlation between size and transfection efficiency: the larger the particle the better the transfection efficiency. This is most likely a size and mass issue. If the particle is larger and heavier, there might be a greater chance that the cell and nanoparticle will be in contact with each other. On the other hand there will be more particles present as the core size gets smaller, with the greatest number of particles present in the DNA only group. With nanoparticles, the smaller the TAP containing nanoparticles, the less streptavidin that will be present and consequently fewer DNA particles will be bound. So, by this formula, increasing the size would decrease the likelihood of transfection because there would be less nanoparticles per given volume. We found the opposite to be the case. One possible scenario is that the addition of multiple TAP copies (47 in the case of MNP) increases the mass of the nanoparticle so much, that the nanoparticles settle to the bottom. More experiments need to be done in order to clarify this issue of size versus transfection efficiency.

The issue of nanoparticle toxicity is an important area of research. One of the more frequent criticisms of MNP in culture and in animals is the toxicity of the nanoparticle. Specifically, the major concern revolves around the hypothesis that the iron in the core of the MNP could induce the formation of ROS, via Fenton cycling or other mechanisms. We have tested this hypothesis with CM-H_2DCFDA and flow cytometry. This experiment demonstrated that the levels of ROS, in MNP-treated cells, were equivalent to those in untreated controls. This experiment confirms our observation that the cells do not seem to be harmed by the penetrating MNP. This is likely due to the fact that the nanoparticles do not readily break down within the cells. Rather, they appear quite stable during the course of these experiments. Although this is very promising, the next step is to evaluate their performance and toxicity in animal models of ROP.

In summary, multilayered nanoparticles can be constructed with reasonable ease in a molecular biology laboratory. These particles have the potential to transfect a multitude of cells, including those isolated from human sources. Tethered nanoparticle transfection has the potential to decrease the possibility of the delivered gene integrating into the host genome. Additionally this technology can increase the stability of the DNA in the cellular milieu. These particles also have benefits over virally delivered genes, like decreased inflammation and immune response, and the MNP do not induce ROS. One limitation of the MNP reported here is that expression is short-term and transfection efficiency is low, when compared to other means of gene delivery (i.e., viral). These shortcomings may be remedied with better cell entry and nuclear localization molecules attached to the surface of the nanoparticle. The nanoparticles investigated offer the possiblity of adding multiple ordered layers. Perhaps the need to better filter out defective nanoparticles in order to increase functionality is also important. If these efforts are successful, the potential reward is huge. The nanoparticle platform is capable of delivering molecular programming to a single cell and dictating its actions toward insults. This behavior modification at a molecular level can be used to prevent disease as it happens. To this end, we are developing a MNP based system to deliver

biosensors to the eye which can detect, react and thereby prevent retinopathy of prematurity [17]. The next step is to deliver nanoparticles to relevant cells that can detect and respond to the initial high oxygen insult that initiates ROP.

ACKNOWLEDGEMENTS

This work was supported by the Biomolecular, Physics and Chemistry Program under NASA grant NAS2-02059 (TP, JS, NW, MM, JL), National Eye Institute grant R03EY013744 (GL), R01EY09357 (GL), EY01765 (Wilmer), and the Johns Hopkins Hematology Training grant T32HL007525 (TP).

REFERENCES

1. Koropchak JA, Sadain S, Yang X, Magnusson LE, Heybroek M, Anisimov M, Kaufman SL. Nanoparticle detection technology for chemical analysis. Anal Chem 1999; 71:386A-394A.
2. Douglas SJ, Davis SS, Illum L. Nanoparticles in drug delivery. Crit Rev Ther Drug Carrier Syst 1987; 3:233-61.
3. Kreuter J, Tauber U, Illi V. Distribution and elimination of poly(methyl-2-14C-methacrylate) nanoparticle radioactivity after injection in rats and mice. J Pharm Sci 1979; 68:1443-7.
4. Panyam J, Labhasetwar V. Biodegradable nanoparticles for drug and gene delivery to cells and tissue. Adv Drug Deliv Rev 2003; 55:329-47.
5. Vijayanathan V, Thomas T, Thomas TJ. DNA nanoparticles and development of DNA delivery vehicles for gene therapy. Biochemistry 2002; 41:14085-94.
6. Benns JM, Kim SW. Tailoring new gene delivery designs for specific targets. J Drug Target 2000; 8:1-12.
7. Hogemann D, Ntziachristos V, Josephson L, Weissleder R. High throughput magnetic resonance imaging for evaluating targeted nanoparticle probes. Bioconjug Chem 2002; 13:116-21.
8. Lanza GM, Yu X, Winter PM, Abendschein DR, Karukstis KK, Scott MJ, Chinen LK, Fuhrhop RW, Scherrer DE, Wickline SA. Targeted antiproliferative drug delivery to vascular smooth muscle cells with a magnetic resonance imaging nanoparticle contrast agent: implications for rational therapy of restenosis. Circulation 2002; 106:2842-7.
9. Sun ML, Zhang H. [The development of nanoparticles on DNA isolation and purification]. Sheng Wu Gong Cheng Xue Bao 2001; 17:601-3.
10. Winter PM, Caruthers SD, Kassner A, Harris TD, Chinen LK, Allen JS, Lacy EK, Zhang H, Robertson JD, Wickline SA, Lanza GM. Molecular imaging of angiogenesis in nascent Vx-2 rabbit tumors using a novel alpha(nu)beta3-targeted nanoparticle and 1.5 tesla magnetic resonance imaging. Cancer Res 2003; 63:5838-43.
11. Albig A. Isolation of mRNA binding proteins using the μMACS Streptavidin Kit. MACS & more 2001; 5:6-7.
12. Violante MR. Potential of microparticles for diagnostic tracer imaging. Acta Radiol Suppl 1990; 374:153-6.
13. Petersein J, Saini S, Weissleder R. Liver. II: Iron oxide-based reticuloendothelial contrast agents for MR imaging. Clinical review. Magn Reson Imaging Clin N Am 1996; 4:53-60.
14. Mitchell DG. MR imaging contrast agents—what's in a name? J Magn Reson Imaging 1997; 7:1-4.
15. Bonnemain B. Superparamagnetic agents in magnetic resonance imaging: physicochemical characteristics and clinical applications. A review. J Drug Target 1998; 6:167-74.
16. Wang YX, Hussain SM, Krestin GP. Superparamagnetic iron oxide contrast agents: physicochemical characteristics and applications in MR imaging. Eur Radiol 2001; 11:2319-31.
17. Prow T, Grebe R, Merges C, Smith JN, McLeod DS, Leary JF, Lutty GA. Nanoparticle tethered antioxidant response element as a biosensor for oxygen induced toxicity in retinal endothelial cells. Mol Vis 2006; 12:616-25.
18. Plank C, Schillinger U, Scherer F, Bergemann C, Remy JS, Krotz F, Anton M, Lausier J, Rosenecker J. The magnetofection method: using magnetic force to enhance gene delivery. Biol Chem 2003; 384:737-47.
19. Krotz F, Sohn HY, Gloe T, Plank C, Pohl U. Magnetofection potentiates gene delivery to cultured endothelial cells. J Vasc Res 2003; 40:425-34.
20. Plank C, Anton M, Rudolph C, Rosenecker J, Krotz F. Enhancing and targeting nucleic acid delivery by magnetic force. Expert Opin Biol Ther 2003; 3:745-58.
21. Plank C, Scherer F, Schillinger U, Bergemann C, Anton M. Magnetofection: enhancing and targeting gene delivery with superparamagnetic nanoparticles and magnetic fields. J Liposome Res 2003; 13:29-32.
22. Krotz F, de Wit C, Sohn HY, Zahler S, Gloe T, Pohl U, Plank C. Magnetofection—a highly efficient tool for antisense oligonucleotide delivery in vitro and in vivo. Mol Ther 2003; 7:700-10.
23. Mamedov AA, Belov A, Giersig M, Mamedova NN, Kotov NA. Nanorainbows: graded semiconductor films from quantum dots. J Am Chem Soc 2001; 123:7738-9.
24. Mullikin JC. Discrete and continuous methods for three-dimensional image analysis [dissertation]. The Netherlands: Delft University of Technology; 1993. p. 47-48.
25. Lutty GA, Mathews MK, Merges C, McLeod DS. Adenosine stimulates canine retinal microvascular endothelial cell migration and tube formation. Curr Eye Res 1998; 17:594-607.
26. Ohki EC, Tilkins ML, Ciccarone VC, Price PJ. Improving the transfection efficiency of post-mitotic neurons. J Neurosci Methods 2001; 112:95-9.

The print version of this article was created on 26 May 2006. This reflects all typographical corrections and errata to the article through that date. Details of any changes may be found in the online version of the article.